Numerical Modelling of Transient Liquid Phase Bonding and Other Diffusion Controlled Phase Changes

ILLINGWORTH T.C.*, GOLOSNOY I.O., GERGELY V. and CLYNE T.W.
Department of Materials Science, University of Cambridge, Pembroke Street, Cambridge, CB2 3QZ, U.K.
*Corresponding author. Email: tci20@cam.ac.uk

ABSTRACT

Diffusion in alloys of inhomogeneous composition can induce phase changes, even at a constant temperature. A transient liquid phase (TLP), in which a liquid layer is formed and subsequently solidifies, is one example of such an isothermal phase change. This phenomenon is exploited industrially in TLP bonding and sintering processes. Successful processing requires understanding of the behaviour of the transient liquid layer in terms of both diffusion-controlled phase boundary migration and capillarity-driven flow.

In this paper, a numerical model is presented for the simulation of diffusion-controlled melting and solidification. The width of the liquid layer, time to solidification and solute concentration profiles are studied for various bonding conditions. A novel approach is proposed, allowing high precision even with coarse meshes and high interface velocities. The model is validated using experimental data from a variety of systems, including solid/solid diffusion couples.

INTRODUCTION

Transient liquid phases (TLPs) are observed in many alloy systems. However, commercial exploitation of the phenomenon is relatively limited. This is partly because current understanding of the process is incomplete, rendering the optimisation of various process variables and design parameters difficult.

Qualitatively, TLPs are easily understood; a full description of the underlying physical processes is given by MacDonald and Eagar [1]. The essential requirement is that the liquidus temperature of an alloy varies with composition. It is then possible for the variation in composition of an inhomogeneous alloy to cause localised melting at temperatures where the bulk of the material remains solid. If liquid and solid of different compositions are in contact, diffusion will change the concentration profile and can cause an initial widening of the liquid layer, followed by solidification, even during an isothermal heat treatment. Such diffusion-controlled solidification can be used to bond particles in a powder compact (TLP sintering) or to join larger objects (TLP bonding).

Once solidified, the final composition in the vicinity of a joint can be relatively homogenous. As a result, its properties (such as strength and remelt temperature) can approach those of the parent material. The transient presence of a liquid phase also affords advantages over other joining techniques. Flow under the influence of capillary forces will naturally tend to eliminate any porosity within a bond, without the need to impose any external pressure. In the case of TLP sintering, the liquid phase can additionally promote particle rearrangement, leading to rapid densification of a green body.

The transience of the liquid phase arises from changes in composition as a result of diffusion. In the next section, the physical processes which underlie TLPs are examined and a model is developed in which they are simulated.

MODELLING

Mathematical description of the problem

Diffusion in both liquid and solid is assumed to be governed by Fick s second law (the Diffusion Equation),

$$\frac{\partial c(x,t)}{\partial t} = \frac{\partial}{\partial x}\left(D(c(x,t))\frac{\partial c(x,t)}{\partial x} \right), \qquad (1)$$

where the composition, $c(x,t)$, is a function of both position (x) and time (t). $D(c(x,t))$ is the diffusion coefficient of solute in either the liquid or solid phase, which depends on both temperature and concentration. The diffusion equation (1) has been solved for a range of initial and boundary conditions. However, TLPs have solid and liquid phases which change size over time; this introduces a moving boundary condition, which complicates the analysis.

[INSERT FIGURE 1]

A one dimensional planar geometry is assumed, as shown in figure 1. The variable $s(t)$ is introduced to describe the position of a solid/liquid interface (which varies as a function of time). The moving boundary problem can then be stated more fully as [2]

$$\frac{\partial c(x,t)}{\partial t} = \frac{\partial}{\partial x}\left(D_A(c(x,t))\frac{\partial c(x,t)}{\partial x} \right), \qquad 0<x<s(t) \qquad (2)$$

$$\frac{\partial c(x,t)}{\partial t} = \frac{\partial}{\partial x}\left(D_B(c(x,t))\frac{\partial c(x,t)}{\partial x} \right), \qquad s(t)<x<\mathrm{L} \qquad (3)$$

$$D_A(c(x,t))\frac{\partial c(x,t)}{\partial x}\bigg|_{x=s(t)^-} - D_B(c(x,t))\frac{\partial c(x,t)}{\partial x}\bigg|_{x=s(t)^+} = \left[c_B - c_A\right]\frac{ds(t)}{dt}. \qquad x=s(t) \qquad (4)$$

The first equation describes diffusion to the left of the interface, in phase A (liquid in the case of figure 1). The second equation refers to diffusion in phase B, to the right of the interface (the solid). The third describes the moving boundary condition at the interface, which is derived by requiring that solute be conserved there. A complete expression of the problem also requires initial conditions, as well as conditions at the fixed boundaries $x=0$ and $x=\mathrm{L}$; these are trivial and are omitted for clarity. Any diffusion-controlled isothermal phase change with a planar geometry will obviously be subject to the same governing equations, irrespective of whether the phases are solid or liquid. The model developed below can thus be applied to solid state transformations, as well as TLPs.

Systems of partial differential equations with moving boundary conditions (also known as Stefan problems) arise in a variety of modelling situations across the sciences [3]. For certain idealised cases, analytical solutions are available [3-5]. In general, however, numerical solution methods are required. Several viable approaches have been proposed. Unfortunately, Furzeland [6] concludes that the most effective approach to solving a Stefan problem depends on the exact nature of the problem itself. Zhou *et al*. [7] describe numerical methods formulated specifically to study TLP problems.

Fixed spatial discretisation models

In modelling TLPs, the main difficulty arises in tracking the motion of solid/liquid interfaces. Previously, a fixed discretisation of the domain x=0 to x=L has generally been imposed, with a certain concentration being associated with each point after every timestep. The motion of the interface can be described in a number of ways.

One approach, used by Nakagawa *et al*. [8] and Cain *et al*. [9], is to solve the diffusion equations by imposing the requirement that the interface be located at one of the discretisation points. In this case, only a stepwise motion of the interface is permitted. Such a constraint is physically unrealistic. In addition, restrictions on the interface position probably introduce significant errors into the model, as inaccurate approximations of the interface position will directly affect estimates of the fluxes there (and will therefore also affect the predicted interface motion).

More refined models explicitly take account of the interface position and use a discretised form of equation (4) to predict its motion. Shinmura *et al*. [10] used an algorithm based on this approach to investigate possible interlayer materials for bonding nickel. Zhou and North [2] also employed this approach. In an attempt to improve the accuracy of their predictions for the interface motion, they additionally proposed the use of a quadratic expression for the concentration profile near the interface, in order to better estimate the fluxes there.

These two models differ slightly in the way that they solve the diffusion equations ((2) and (3)): Shinmura *et al*. [10] use an explicit expression, whereas Zhou and North [2] claim to use an implicit scheme. Certainly, they solve an implicit form of equations (2) and (3). However, the three equations (2)-(4) are interdependent - implicit methods of calculating future concentration profiles will therefore give rise to expressions involving future interface positions as well as future concentrations. Since their method calculates future interface positions by solving (4) explicitly, their scheme is only semi-implicit overall. As a result, there is a limitation on the size of timestep that can be used to generate a solution.

Sinclair *et al*. [11] also implemented an explicit version of this same algorithm and used it to investigate the solidification of ternary systems. TLP bonding of systems with three components has been investigated in parallel by Campbell and Boettinger [12]. They used generic software, which was developed to describe general diffusion-controlled transformations (not TLP bonding specifically).

It is relatively simple to derive finite difference approximations of the governing equations (2)-(4) if a fixed discretisation of space is imposed. Nevertheless, numerical solutions must be calculated carefully. In particular, during timesteps when the interface moves from one element to its neighbour, schemes developed for fixed meshes will not generally conserve solute. Modifications to ensure the conservation of solute are possible, but they increase the complexity of programming. If the interface moves more than one element, solute conservative programming becomes even more difficult.

Unfortunately, rapid interface motion is typical of the early stages of TLP bonding. In order to minimise inaccuracies associated with the non-conservation of solute, small timesteps must be used to model dissolution. At later times, however, the rate of solidification is determined by diffusion in the solid (rather than diffusion in the liquid). Interface velocities are therefore much lower. This difference means that, if the timestep is fixed in such a way as to limit errors due to non-

conservation during dissolution, large amounts of computing time will be required to model the complete solidification stage too. The use of variable timesteps to model the different stages of the process is one way of overcoming this problem, although a constant timestep was used in each of the models described above. No reasons are given in any of the reports for choosing a particular value of _t and the question of solute conservation is nowhere addressed. In particular, it is not clear how the accuracy of predictions is affected by the non-conservation of solute.

For diffusion couples in which both sides are solid, interface velocities do not vary to the same extent. The use of constant timesteps is therefore appropriate for non-conservative models of solid-state diffusion-controlled phase changes. However, if such models are to be extended to encompass solid/liquid interactions, timestep selection becomes an important issue. For conservative discretisation schemes, the error is determined solely by truncation errors. The way in which the timestep affects the accuracy of the model will, therefore, be clearer.

Use of variable spatial discretisation

Instead of tracking the motion of a moving boundary across a constant spatial discretisation, one alternative is to impose a transformation that fixes the interface [3]. This approach was used by Tanzilli and Heckel to model solid-state phase transformations as long ago as 1968 [13]. They suggest that it would be beneficial to re-mesh after each timestep to take account of the moving boundary. It would then be possible to allow the interface to move in an unconstrained manner, while still ensuring that its position always coincides with a discretisation point. Kajihara and Kikuchi [14] used an implicit version of the same model to investigate the behaviour of solid $\gamma/\alpha/\gamma$ diffusion couples in the Fe-Cr-Ni system.

This type of approach is adopted in the present work. To impose a variable space grid on the simulation, a wholesale co-ordinate transformation is introduced. An implicit 1-D model which describes the phase changes associated with TLP bonding (or indeed any other diffusion controlled phase change) is then developed in such a way as to ensure the conservation of solute.

The variable space grid is achieved by introducing two new positional variables: $u(t) = \frac{x}{s(t)}$ and $v(t) = \frac{x - s(t)}{L - s(t)}$. These definitions mean that, for any time, the interval $0<x<s(t)$ coincides with $0<u<1$, and that $s(t)<x<L$ coincides with $0<v<1$. Changing co-ordinate system also means that the governing equations (2)-(4) must be modified. Writing $p(u,t)$ as the concentration in phase A (which coincides with $c(x,t)$ in $0<x< s(t)$) and $q(v,t)$ as the concentration in phase B (corresponding to $c(x,t)$ in $s(t)<x<L$), equations (2)-(4) become [3]:

$$s(t)^2 \frac{\partial p(u,t)}{\partial t} - us(t)\frac{ds(t)}{dt}\frac{\partial p(u,t)}{\partial u} = \frac{\partial}{\partial u}\left(D_A(p(u,t))\frac{\partial p(u,t)}{\partial u}\right), \qquad 0<u<1 \qquad (5)$$

$$\left[L - s(t)\right]^2 \frac{\partial q(v,t)}{\partial t} - (1-v)\left[L - s(t)\right]\frac{ds(t)}{dt}\frac{\partial q(v,t)}{\partial v} = \frac{\partial}{\partial v}\left(D_B(q(v,t))\frac{\partial q(v,t)}{\partial v}\right), \qquad 0<v<1 \qquad (6)$$

$$\frac{D_A(p(u,t))}{s(t)}\frac{\partial p(u,t)}{\partial u}\bigg|_{u=1} - \frac{D_B(q(v,t))}{L - s(t)}\frac{\partial q(v,t)}{\partial v}\bigg|_{v=0} = \left[c_B - c_A\right]\frac{ds(t)}{dt}. \qquad u=1;\ v=0 \qquad (7)$$

In this new co-ordinate system, the interface is *fixed* at u=1 and v=0 for all t. Fixing the front in this way means that interface motion can be handled more easily. On the other hand, the derivation of a finite difference scheme that conserves solute becomes more involved.

Using the identities $\frac{\partial(pu)}{\partial u} = p + u\frac{\partial p}{\partial u}$ and $\frac{\partial(ps)}{\partial t} = p\frac{ds}{dt} + s\frac{\partial p}{\partial t}$, equation (5) can be re-written in divergent form as

$$\frac{\partial\left(ps\right)}{\partial t} = \frac{ds}{dt}\frac{\partial\left(pu\right)}{\partial u} + \frac{1}{s}\frac{\partial}{\partial u}\left(D_A\frac{\partial\left(pu\right)}{\partial u}\right). \qquad 0<u<1 \qquad (8)$$

Similarly, (6) can be expressed as

$$\frac{\partial\left(q\left[L-s\right]\right)}{\partial t} = \frac{ds}{dt}\frac{\partial\left(q\left[1-v\right]\right)}{\partial v} + \frac{1}{L-s}\frac{\partial}{\partial v}\left(D_B\frac{\partial\left(qv\right)}{\partial v}\right). \qquad 0<v<1 \qquad (9)$$

Discretising the space co-ordinate u at N points (u_0 $u_{N\text{-}1}$), writing $u_{i\pm 1/2}$ as the position midway between u_i and u_{i-1} and introducing the timestep δt such that $t^{j+1} = t^j + \delta t$, the finite volume technique [15] is used to integrate (8) over one spacestep and one timestep:

$$\int_{u_{i-1/2}}^{u_{i+1/2}}\int_{t^j}^{t^{j+1}}\frac{\partial\left(ps\right)}{\partial t}dtdu = \int_{t^j}^{t^{j+1}}\int_{u_{i-1/2}}^{u_{i+1/2}}\frac{ds}{dt}\frac{\partial\left(pu\right)}{\partial u} + \frac{1}{s}\frac{\partial}{\partial u}\left(D_A\frac{\partial\left(pu\right)}{\partial u}\right)dudt. \qquad 0<u<1 \qquad (10)$$

Introducing $p_i^{j+\sigma}$ (and $s^{j+\sigma}$) to represent the concentration at u_i (and the interface position) after a proportion σ of the timestep has elapsed, it follows that

$$\left(p_i^{j+1}s^{j+1} - p_i^j s^j\right)\left(\frac{u_{i+1}-u_{i-1}}{2}\right) =$$
$$\frac{\delta t}{s^{j+\sigma}}\left(\left(D_A\right)_{i+1/2}^{j+\sigma}\frac{p_{i+1}^{j+\sigma}-p_i^{j+\sigma}}{u_{i+1}-u_i} - \left(D_A\right)_{i-1/2}^{j+\sigma}\frac{p_i^{j+\sigma}-p_{i-1}^{j+\sigma}}{u_i-u_{i-1}}\right) + \left(s^{j+1}-s^j\right)\left(p_{i+1/2}^{j+\sigma}u_{i+1/2} - p_{i-1/2}^{j+\sigma}u_{i-1/2}\right), \qquad (11)$$

where $\left(D_A\right)_{i\pm 1/2}^{j+\sigma}$ correspond to the diffusion coefficients for the concentrations mid-way between discretisation points. In the remainder of this work, diffusion coefficients will be assumed to be independent of concentration. For a fixed bonding temperature, $\left(D_A\right)_{i\pm 1/2}^{j+\sigma}$ will be therefore be constant, which will be denoted D_A.

Setting i=1 N-2, equation (11) can be used to generate a set of finite difference approximations for the future compositions in phase A. For i=0 or N-1, finite difference approximations for the relevant boundary conditions must be applied. At the moving interface (u=1), local equilibrium requires that $p_{N-1}^{j+1} = c_A$. At the fixed boundary (u=0), standard techniques [15, 16] can be used to modify (11) so as to ensure zero flux. Doing so gives rise to the finite difference expression

$$\left(p_0^{j+1}s^{j+1} - p_0^j s^j\right)\left(\frac{u_1}{2}\right) = \frac{D_A\delta t}{s^{j+\sigma}}\left(\frac{p_1^{j+\sigma}-p_0^{j+\sigma}}{u_1}\right) + \left(s^{j+1}-s^j\right)\left(p_{1/2}^{j+\sigma}u_{1/2}\right).$$

Similarly, integration can be used to generate finite difference expressions for future compositions in phase B from equation (9):

$$\left(q_i^{j+1}\left(L-s^{j+1}\right)-q_i^j\left(L-s^j\right)\right)\left(\frac{v_{i+1}-v_{i-1}}{2}\right)=$$

$$\frac{\delta t}{L-s^{j+\sigma}}\left(\left(D_B\right)_{i+\frac{1}{2}}^{j+\sigma}\frac{q_{i+1}^{j+\sigma}-q_i^{j+\sigma}}{v_{i+1}-v_i}-\left(D_B\right)_{i-\frac{1}{2}}^{j+\sigma}\frac{q_i^{j+\sigma}-q_{i-1}^{j+\sigma}}{v_i-v_{i-1}}\right)+\left(s^{j+1}-s^j\right)\left(q_{i+\frac{1}{2}}^{j+\sigma}\left(1-v_{i+\frac{1}{2}}\right)-q_{i-\frac{1}{2}}^{j+\sigma}\left(1-v_{i-\frac{1}{2}}\right)\right) \tag{12}$$

Again, the simplifying assumption that $\left(D_B\right)_{i+\frac{1}{2}}^{j+\sigma}=\left(D_B\right)_{i-\frac{1}{2}}^{j+\sigma}=D_B$ is made. Appropriate boundary conditions are easily derived in the same way as for phase A.

Equation (7), which describes the motion of the interface, remains to be discretised. The derivation of equation (7) followed from the requirement that matter be conserved. A discretised form is generated in the same way. Consider the total amount of solute in the system at time t^j:

$$s^j\left[p_0^j\frac{u_1-u_0}{2}+\sum_{i=1}^{N-2}p_i^j\frac{u_{i+1}-u_{i-1}}{2}+p_{N-1}^j\frac{u_N-u_{N-1}}{2}\right]$$

$$+\left(L-s^j\right)\left[q_0^j\frac{v_1-v_0}{2}+\sum_{i=1}^{M-2}q_i^j\frac{v_{i+1}-v_{i-1}}{2}+q_{M-1}^j\frac{v_M-v_{M-1}}{2}\right].$$

At time t^{j+1}, the total amount of solute is given by

$$s^{j+1}\left[p_0^{j+1}\frac{u_1-u_0}{2}+\sum_{i=1}^{N-2}p_i^{j+1}\frac{u_{i+1}-u_{i-1}}{2}+p_{N-1}^{j+1}\frac{u_N-u_{N-1}}{2}\right]$$

$$+\left(L-s^{j+1}\right)\left[q_0^{j+1}\frac{v_1-v_0}{2}+\sum_{i=1}^{M-2}q_i^{j+1}\frac{v_{i+1}-v_{i-1}}{2}+q_{M-1}^{j+1}\frac{v_M-v_{M-1}}{2}\right].$$

For the model to be conservative, the difference between these two values must be zero. Subtracting the first expression from the latter gives rise to terms such as $\frac{u_{i+1}-u_{i-1}}{2}\left[s^{j+1}p_i^{j+1}-s^jp_i^j\right]$, for which alternative expressions are available (equations (11) and (12)). Upon substitution, massive cancellation occurs, resulting in the following finite difference expression for (7):

$$\frac{D_B\delta t}{L-s^{j+\sigma}}\left(\frac{q_1^{j+\sigma}-c_B}{v_1}\right)-\frac{D_A\delta t}{s^{j+\sigma}}\frac{c_A-p_{N-2}^{j+\sigma}}{1-u_{N-2}}=$$

$$\left(s^{j+1}-s^j\right)\left[\frac{1+u_{N-2}}{2}p_{N-1-\frac{1}{2}}^{j+\sigma}+\frac{1-u_{N-2}}{2}c_A-\left(1-\frac{v_1}{2}\right)q_{\frac{1}{2}}^{j+\sigma}-\frac{v_1}{2}c_B\right]. \tag{13}$$

Equations (11)-(13) form a complete finite difference expression for the problem described analytically in equations (5)-(7). The way in which they were derived has ensured that they conserve solute. Appropriate approximations for terms at intermediate times ($j+\sigma$) and intermediate positions ($i\pm\frac{1}{2}$) will be considered presently, along with efficient methods of solving the resulting set of equations.

Implementation

The problems relating to diffusion ((11) and (12)) and interface motion (13) are interdependent: the diffusion equations depend on the future interface position. Conversely, for all implicit schemes ($\sigma \neq 0$), the interface equation involves terms which depend on future concentrations. The concentration profiles and the interface motion therefore form a strongly coupled problem. The equations cannot be solved independently; instead, they must be solved simultaneously.

A further difficulty is that the system of simultaneous equations is non-linear, so an iterative solution method must be used. This is potentially very demanding in terms of computing time. But careful analysis can significantly improve the efficiency of the algorithm.

Firstly, note that it is trivial to solve equation (13) for s^{j+1} if estimates are available for $s^{j+\sigma}$ and concentrations profiles $p_i^{j+\sigma}$ and $q_i^{j+\sigma}$ (from which intermediate concentration profiles $p_{i\pm 1/2}^{j+\sigma}$ and $q_{i\pm 1/2}^{j+\sigma}$ can be determined). Once s^{j+1} is known, it is easy to find future concentrations p_i^{j+1}: assuming that terms such as $p_{i\pm 1/2}^{j+\sigma}$ can be approximated sufficiently well using only the concentrations of neighbouring points at the same time (i.e. $p_{i-1}^{j+\sigma}$, $p_i^{j+\sigma}$ and $p_{i+1}^{j+\sigma}$), equation (11) is reduced to a tridigonal form, which is easily inverted. Concentrations in phase B can also be calculated by inverting a tridiagonal matrix which follows from (12).

Having decoupled and linearised the problem in this way, implementation is simple. The results discussed in the following section have been generated by an algorithm which, at each timestep, executes the following procedure:

1) Take s^j, p_i^j and q_i^j as initial values for $s^{j+\sigma}$, $p_i^{j+\sigma}$ and $q_i^{j+\sigma}$ and calculate intermediate concentration profiles $p_{i+1/2}^{j+\sigma}$ and $q_{i+1/2}^{j+\sigma}$.
2) Calculate the future interface position, s^{j+1} using (13).
3) Using this value of s^{j+1}, update the estimate for $s^{j+\sigma}$.
4) Calculate the future interface positions, p_i^{j+1} and q_i^{j+1} for all *i* using (11), (12) and the boundary conditions.
5) Using these values for p_i^{j+1} and q_i^{j+1}, update the estimates for $p_i^{j+\sigma}$ and $q_i^{j+\sigma}$ and calculate intermediate concentration profiles $p_{i+1/2}^{j+\sigma}$ and $q_{i+1/2}^{j+\sigma}$.

Steps 2)-5) are then repeated until successive estimates of the interface position s^{j+1} differ by less than some fixed tolerance. If successive refinements do indeed converge to some fixed value, this will correspond to a solution of the implicit set of discretised equations.

It is well known [16, 17] that the Crank-Nicolson scheme ($\sigma = 1/2$) gives an error that is proportional to δt^2. This would seem preferable the fully implicit scheme ($\sigma = 1$), which generates

errors proportional to δt. However, if the Crank-Nicolson scheme is used to discretise discontinuous composition profiles, unphysical oscillations will be predicted close to the discontinuity unless the timestep is of the order of $\frac{h^2}{\max\left(D_A, D_B\right)}$ (where h is the spacestep) [16]. On the other hand, fully implicit schemes predict monotonic concentration profiles, no matter what timestep is chosen [15-17]. Since discontinuous concentration profiles and large diffusion coefficients are inherent to TLPs, we limit our attention to fully implicit schemes.

Monotonicity concerns must also be taken into account when considering possible approximations for the intermediate concentrations $p_{i\pm 1/2}^{j+\sigma}$ and $q_{i\pm 1/2}^{j+\sigma}$. It is known that second-order centre-difference schemes can produce non-monotonic (oscillating) solutions [15, 17]. In the case of the current problem, trials have indicated that such approximations do indeed generate such unphysical predictions for the TLP problem. Instead, the following fully implicit up/down-wind approximations are used:

- For a positive velocity ($s^{j+1} > s^j$):
  $p_{i+1/2}^{j+\sigma} = p_{i+1}^{j+1}$, $p_{i-1/2}^{j+\sigma} = p_i^{j+1}$ and $q_{i+1/2}^{j+\sigma} = q_{i+1}^{j+1}$, $q_{i-1/2}^{j+\sigma} = q_i^{j+1}$;
- For a negative velocity ($s^{j+1} < s^j$):
  $p_{i+1/2}^{j+\sigma} = p_i^{j+1}$, $p_{i-1/2}^{j+\sigma} = p_{i-1}^{j+1}$ and $q_{i+1/2}^{j+\sigma} = q_i^{j+1}$, $q_{i-1/2}^{j+\sigma} = q_{i-1}^{j+1}$.

Computer code implementing an algorithm using these approximations has been prepared. Experiments have shown that predictions using these first order approximations for the spatial and temporal variation of composition generates smooth, monotonic profiles. In addition, successive estimates of interface positions at each timestep do indeed converge to fixed values, indicating that linearisating and decoupling the problem is a suitable method of finding its solution in an efficient way. Results from the model are presented in the next section.

VALIDATION, RESULTS AND DISCUSSION

Interface motion has been calculated for a variety of systems. Results agree well with experimental data. In figure 2, the half width of the liquid layer is plotted as a function of time for a Ni-P interlayer between pure Ni plates. Following Zhou and North [2], a constant molar volume is assumed (irrespective of phase and composition)[1]. Experimental data and model predictions from the same source are also presented in figure 2, for comparison with the present work. Initial conditions used in the simulation represent a fully liquid interlayer, whose width is the same as that of the solid material from which it has formed.

[INSERT FIGURE 2]

The behaviour of the transient liquid phase predicted by both models is in accordance with our qualitative understanding of the process. The output is also in approximate quantitative agreement with experimental data, even if very few discretisation points are used.

[1] This assumption will be made in all subsequent calculations.

Both models assume that the number of atoms in any given volume does not vary with composition. Since phosphorous is an interstitial element in solid nickel, this assumption is not strictly correct. However, the very low solidus concentration at the bonding temperature (0.17 at% P) means that errors arising due to this simplification are probably not significant. Assuming a constant molar volume permits the theoretical maximum liquid layer thickness to be calculated — the thickness at which liquid is diluted to the equilibrium concentration, without any diffusion of solute into the solid. For 12.5 m of Ni-19 at% P dissolving pure Ni until it reaches a concentration of 10.2 at% P (the liquidus concentration at the bonding temperature), the theoretical maximum liquid width is 23.2 μm. The predictions of Zhou and North [2] exceed this value, indicating that their simulation does not conserve solute. The predictions of the present model do not exceed the theoretical maximum, which is consistent with the fact that it does conserve solute.

One experimental datum is also greater than the 'theoretical maximum'. This may be because the assumption of constant molar volume in the liquid is incorrect. Alternatively, liquid flow during experiments may have affected the liquid layer, as well as diffusion.

Difficulties associated with eliminating liquid flow mean that experimental data for the width of TLPs that are strictly controlled by diffusion are sparse [1]. If neither phase in a diffusion couple is fluid, flow is not a problem. Data for two-phase diffusion-controlled phase transformations in the solid state are more readily available; since these represent mathematically identical problems, this data can be used to further test the model. Heckel *et al*. [18] investigated the diffusion of Zn in α-β brass diffusion couples. Their data tracking interface positions as a function of time are presented in figure 3 for two different initial thicknesses of β brass (381μm and 762 μm).

[INSERT FIGURE 3]

There is some disagreement in the literature regarding the frequency factors (A) and activation energies (Q) for the diffusion of zinc in Zn-rich α brass at 870˚ßC. Simulations were completed using two different diffusion coefficients, calculated using the published reference values [19]: either $A=0.016\,^{\circ}cm^{2}{}^{\circ}s^{-1}$ and $Q=124.5\,^{\circ}kJ\,^{\circ}mol^{-1}$; or $A=1.7\,^{\circ}cm^{2}{}^{\circ}s^{-1}$ and $Q=172.9\,^{\circ}kJ\,^{\circ}mol^{-1}$. For a temperature of 870˚ßC, these values correspond to diffusion coefficients $D=1.4\times10^{-8}\,^{\circ}cm^{2}{}^{\circ}s^{-1}$ and $D=2.5\times10^{-8}\,^{\circ}cm^{2}{}^{\circ}s^{-1}$. In the β phase, the diffusion coefficient was calculated to be $1.4\times10^{-6}\,^{\circ}cm^{2}{}^{\circ}s^{-1}$ using the undisputed reference values for A and Q.

The simulations using either set of diffusion coefficients qualitatively match the data; and there is close quantitative agreement with the first model. The difference between the two sets of predictions indicates that user-specified diffusion coefficients have a significant effect on the output of the model, as expected. Clearly, correct diffusion coefficients are required for accurate predictions. The use of concentration-dependent diffusion coefficients might significantly improve the accuracy of the model. However, on account of the paucity of data corresponding to the concentration-dependency of diffusion coefficients in most systems, such an extension has not been attempted.

For certain special cases, equations (2)-(4) can be treated analytically - see the reviews of Zhou [4] and Liu *et al*. [5]. One such case is the solidification of a homogenous liquid at composition c_A with an infinitely thick solid of composition c acting as a sink for the solute. The diffusion equation (1) is known to have solutions with the general form $c(x,t) = c_1 + c_2 erfc\left(\frac{x}{2\sqrt{Dt}}\right)$ for some constants c_1 and c_2. $erfc(z)$ is the complementary error function, defined as

$erfc(z) = 1 - erf(z) = \frac{2}{z}\int_z^\infty e^{-r^2} dr$. In the particular case described above, the concentration in the solid infinitely far away from the interface must remain fixed at the initial concentration. One of the constants can be therefore determined immediately: $c_1 = c(\infty, t) = c_\infty$. The other boundary condition in the solid phase, that the concentration at the interface must be fixed at the equilibrium concentration, gives rise to the requirement that $c_B = c_\infty + c_2 erfc\left(\frac{s(t)}{2\sqrt{Dt}}\right)$. Because this relationship must hold for all time, $s(t)$ necessarily varies with $\sqrt{t}$. We shall write $s(t) = k * 2\sqrt{Dt}$ for some constant k. Requiring that solute be conserved (equation (7)) means that k must satisfy $\sqrt{\pi} * k \exp\left(k^2\right) erfc(k) = \frac{c_A - c_\infty}{c_A - c_B}$. Solving for k, it is possible to calculate c_2 and the solution to the problem is complete.

With numerical models, it is not possible to represent a solute sink of infinite extent. But if the diffusion coefficient in the solid is 4.8×10^{-8} cm^{2}s^{-1}, significant diffusion of solute to a position 10 cm from the interface will take a very long time. We therefore approximate the infinite case described by the analytical solution by setting $s(0)$=1cm and L=10cm to generate comparable numerical solutions, shown in figure 4.

[INSERT FIGURE 4]

The main errors in the numerical predictions arise at small times, when large concentration gradients are present in the system. Later, when the composition gradients are less sharp, the interface velocities predicted by all the different discretisations schemes (the gradient of the lines in figure 4) are very similar (and are in close agreement with analytical predictions). For a uniform discretisation, concentrations that change rapidly with position will obviously be better described by a finer mesh. Indeed, errors in the predicted interface position when each phase is discretised at 250 points are much smaller than errors generated when 25 points are used. In fact, decreasing the stepsize by a factor of 10 reduces the error by a factor of 10 (for sufficiently small timesteps). In other words, the model is first order accurate in space. Other simulations in which the discretisation of u and v is fixed and the timestep varies indicate that the model is also first order accurate in time.

Because front fixing methods discretise each phase separately, it is possible to introduce non-uniform meshes. In particular, it is possible to have finer spatial resolution in regions with large concentration gradients (near the interface, for example) and larger spacesteps elsewhere. The dashed line represents the predicted interface motion for just such a discretisation, and one with only 25 points. Errors in the calculated interface position are greatly reduced by the introduction of a non-uniform mesh.

CONCLUSIONS

A model has been developed to describe isothermal phase changes that are controlled by the diffusion of matter under the assumptions that

1) There is local equilibrium at the interfaces;
2) Diffusion of matter can be described by Fick s second law.

The implementation considered in the present work models a two-phase diffusion couple in one dimension (describing a planar geometry). Only binary systems have been considered in the present work, and the diffusion coefficient in each phase is assumed to be independent of composition. None of these conditions are requirements of the method: extensions to cover many phases in higher dimensions, or several components and variable diffusion coefficients are possible.

The numerical scheme requires a system of coupled non-linear equations to be solved. The implementation described above is fully implicit and decouples the problem into a set of linear equations which are solved iteratively. Calculations have been found to converge to accurate solutions, even with large timesteps. Large spacesteps can also be used with this method, as can non-uniform meshes. Because the discretisation moves with the interface, the use of appropriate non-uniform meshes can significantly improve model predictions.

Validation of the model has been possible using experimental data from various systems, including TLP and solid-state diffusion couples. Agreement between model and observation is good, even for relatively large steps in space and time. In contrast with previous models of diffusion-controlled phase changes, our scheme also conserves solute. It has first order accuracy in space and time.

The model has been implemented in the C programming language; optimising the efficiency of the code means that calculations can be completed very rapidly. The code is freely available to download from the Materials Algorithm Project web-site: http://www.msm.cam.ac.uk/MAP

1. MacDonald, W. and T.W. Eagar, *Transient Liquid Phase Bonding.* Ann. Rev. Mat. Sci., 1992. **22**: p. 23-46.
2. Zhou, Y. and T.H. North, *Kinetic modelling of diffusion-controlled, two-phase moving interface problems.* Modelling Simul. Mater. Sci. Eng., 1993. **1**(4): p. 505-516.
3. Crank, J., *Free and Moving Boundary Problems*. 1984, Oxford, UK: Clarendon Press.
4. Zhou, Y., *Analytical modeling of isothermal solidification during transient liquid phase (TLP) bonding.* Journal of Materials Science Letters, 2001. **20**(9): p. 841-844.
5. Liu, S., D.L. Olson, G.P. Martin and G.R. Edwards, *Modeling of Brazing Processes That Use Coatings and Interlayers.* Welding Journal, 1991. **70**(8): p. S207-S215.
6. Furzeland, R.M., *A Comparitive Study of Numerical Methods for Moving Boundary Problems.* J. Inst. Maths Applics, 1980. **26**: p. 411-429.
7. Zhou, Y., W.F. Gale and T.H. North, *Modelling of Transient Liquid Phase Bonding.* Int. Mater. Rev., 1995. **40**: p. 181-196.
8. Nakagawa, H., C.H. Lee and T.H. North, *Modeling of Base-Metal Dissolution Behavior During Transient Liquid-Phase Brazing.* Metallurgical Transactions a-Physical Metallurgy and Materials Science, 1991. **22**(2): p. 543-555.
9. Cain, S.R., J.R. Wilcox and R. Venkatraman, *A diffusional model for transient liquid phase bonding.* Acta Materialia, 1997. **45**(2): p. 701-707.
10. Shinmura, T., K. Ohsasa and T. Narita, *Isothermal solidification behavior during the transient liquid phase bonding process of nickel using binary filler metals.* Materials Transactions Jim, 2001. **42**(2): p. 292-297.
11. Sinclair, C.W., G.R. Purdy and J.E. Morral, *Transient liquid-phase bonding in two-phase ternary systems.* Metallurgical and Materials Transactions a-Physical Metallurgy and Materials Science, 2000. **31**(4): p. 1187-1192.
12. Campbell, C.E. and W.J. Boettinger, *Transient liquid-phase bonding in the Ni-Al-B system.* Metallurgical and Materials Transactions a-Physical Metallurgy and Materials Science, 2000. **31**(11): p. 2835-2847.

13. Tanzilli, R.A. and R.W. Heckel, *Numerical Solutions to the Finite, Diffusion-Controlled, Two-Phase, Moving-Interface Problem (with Planar, Cylindrical, and Spherical Interfaces).* Trans A.I.M.E., 1968. **242**: p. 2312-2321.
14. Kajihara, M. and M. Kikuchi, *Numerical-Analysis of Dissolution of Alpha-Phase in Gamma/Alpha/Gamma-Diffusion Couples of the Fe-Cr-Ni System.* Acta Metallurgica Et Materialia, 1993. **41**(7): p. 2045-2059.
15. Rappaz, M., M. Bellet and M. Deville, *Numerical Modeling in Materials Science and Engineering*. Springer Series in Computational Mathematics. 2003, Berlin: Springer-Verlag.
16. Samarskii, A.A. and P.N. Vabishevich, *Computational heat transfer. V.1. Mathematical Modelling.* 1995, Chichester: Wiley. 406.
17. Tannehill, J.C., D.A. Anderson and R.H. Pletcher, *Computational Fluid Meechanics and Heat Transfer*. 2nd ed. 1997, Washington, London: Taylor & Francis. 792.
18. Heckel, R.W., A.J. Hickl, R.J. Zaehring and R.A. Tanzilli, *Transient Growth of Second Phases During Solution Treatment.* Met. Trans., 1972. **3**: p. 2565-2569.
19. Smithell, *Smithell's Metals Reference book*. 7th ed. 1993: Butterworth.

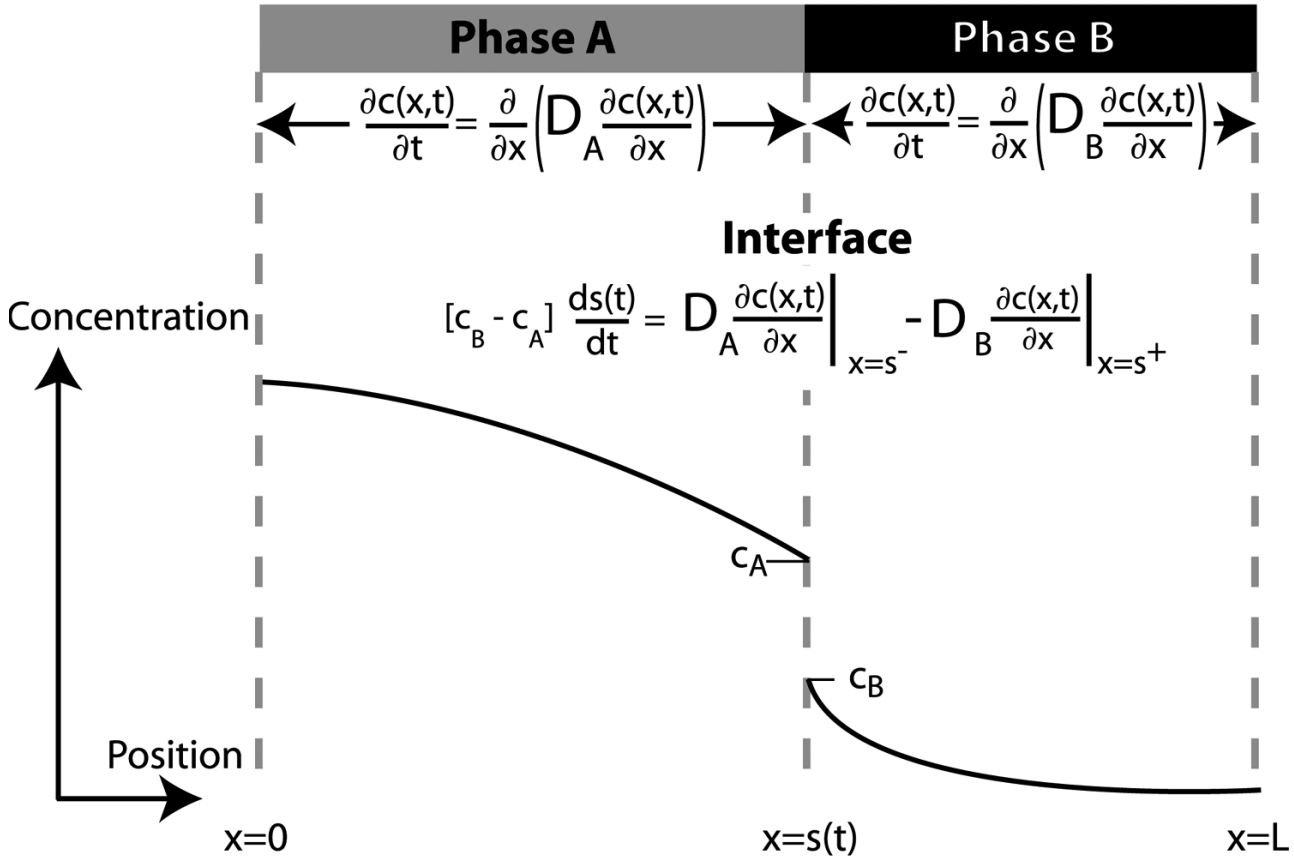

FIGURE 1: Schematic diagram showing a concentration profile across a TLP bond at a particular time t. Only half of the joint is shown; the other half (from x=-L to x=0) will be symmetrical.

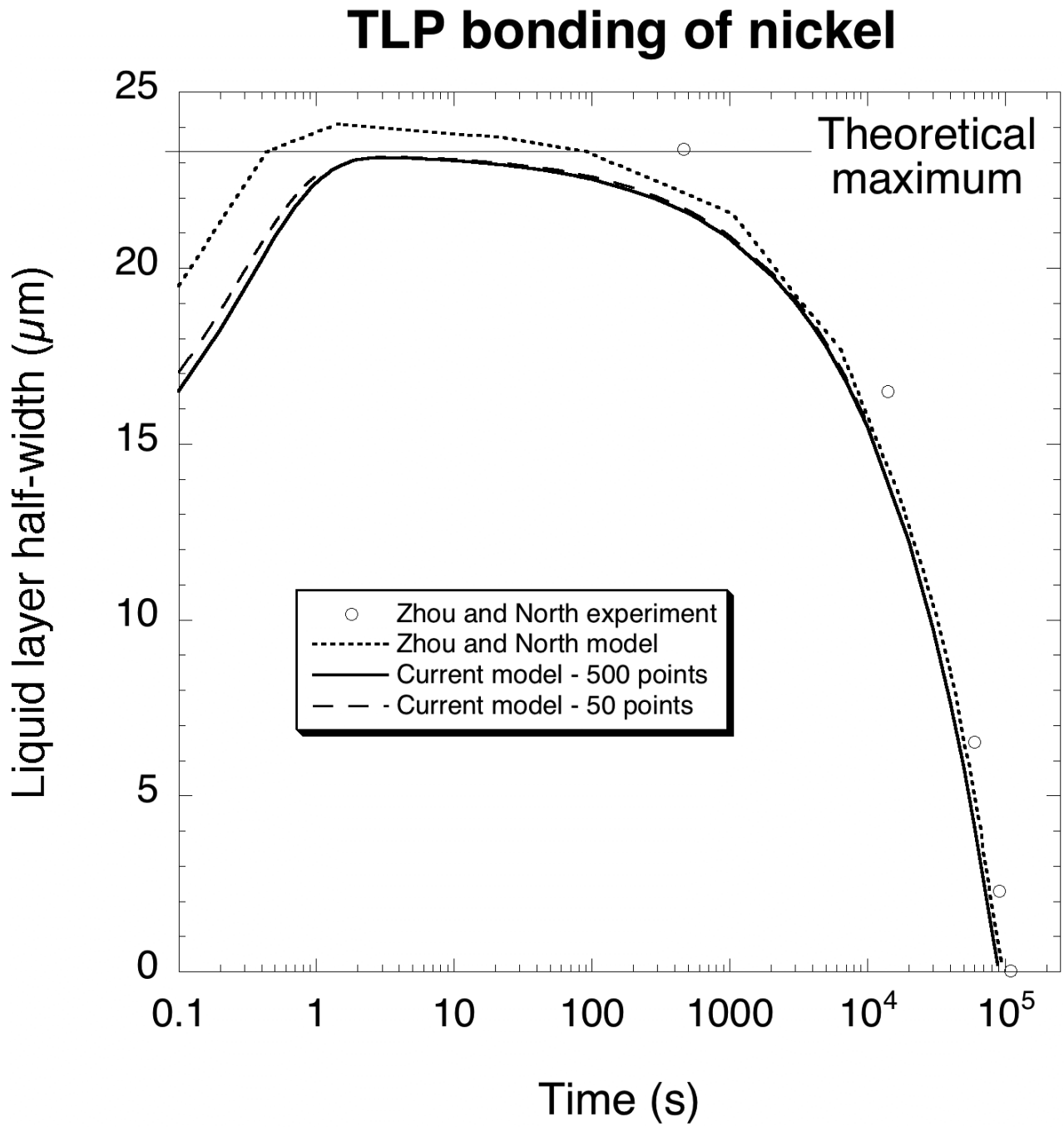

FIGURE 2: Predicted variation of liquid half-layer thickness with time as 25 μm *of liquid at an initial concentration of* Ni19at% P *is placed between two sheet of pure* Ni *each of which is* 6 cm *thick. Experimental data and numerical predictions of Zhou and North [2] are compared with output from the current model, using the same diffusion coefficient for phosphorus in solid and liquid nickel (*1.8×10^{-7} *and* 5×10^{-6} cm^2s^{-1} *respectively). Results for the new model were generated using a timestep of* 0.1 *seconds and by discretising space in* 500 *places (*250 *points in each phase). Under the assumption that the molar volume is constant, it is possible to calculate the ' theoretical maximum liquid layer thickness' by neglecting fluid flow and diffusion in the solid. An experimental datum exceeds this value, possibly because there has been some flow of liquid. Predictions from previous models also exceed the maximum, confirming that the front-tracking model does not conserve solute. The front-fixing model has been developed in such a way as to ensure the conservation of solute, so its predictions do not exceed the maximum.*

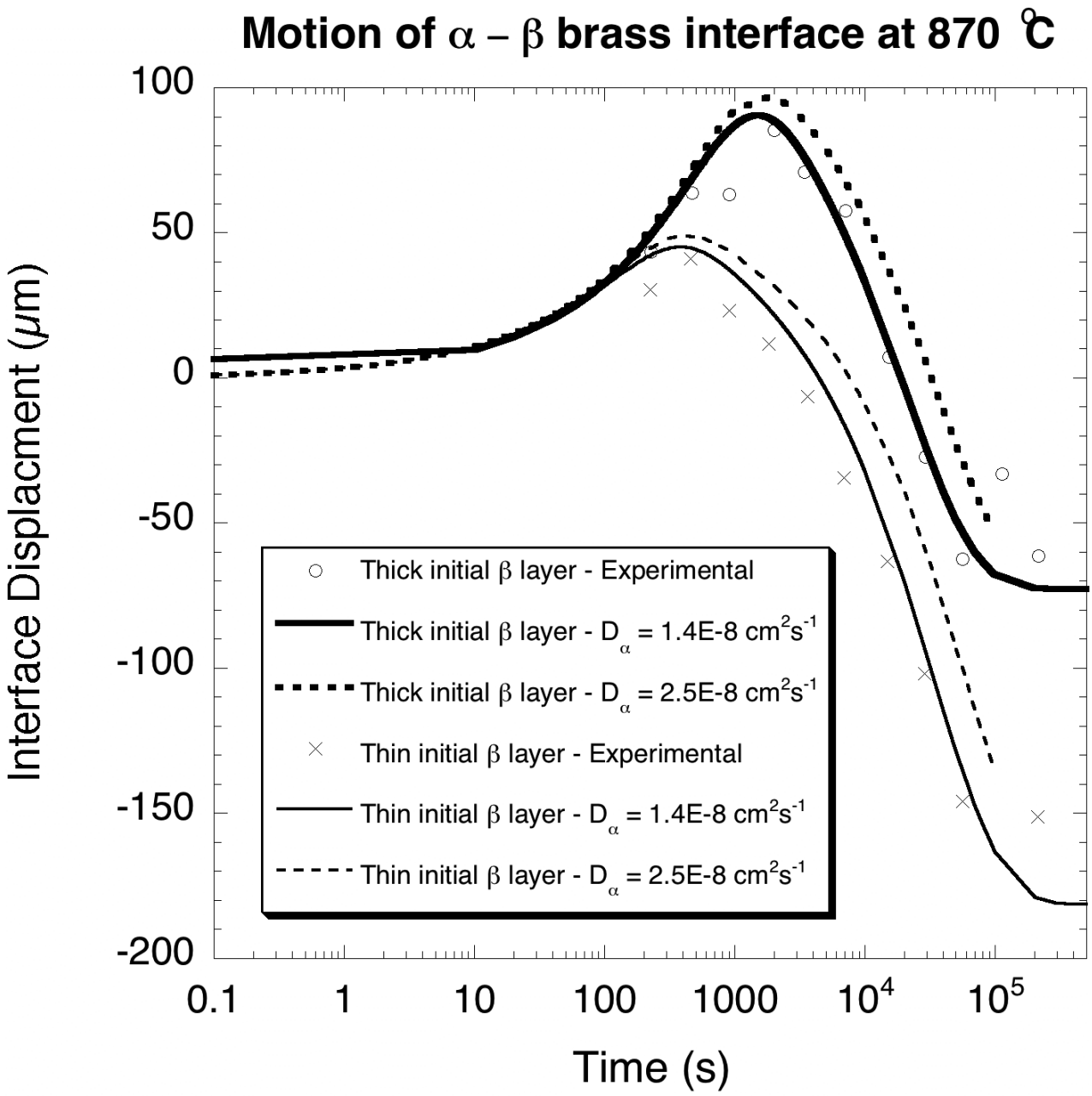

FIGURE 3: Experimental data and model predictions for the growth and subsequent shrinkage of β*-brass in contact with* α*-brass at* 870˚ßC *Experimental data are from Heckel et al. [18], who used a constant thickness of* α*-brass (*749 μm*) and two different thicknesses of* β*-brass (*381 μm *and* 762 μm*) to investigate the motion of a phase boundary in this system. For each initial geometry, two corresponding predictions are plotted — the value of the diffusion coefficient ofZn in* α*-brass is unclear (see text). Predictions were calculated using a timestep of* 10 sec *and* 250 *points to discretise each phase.*

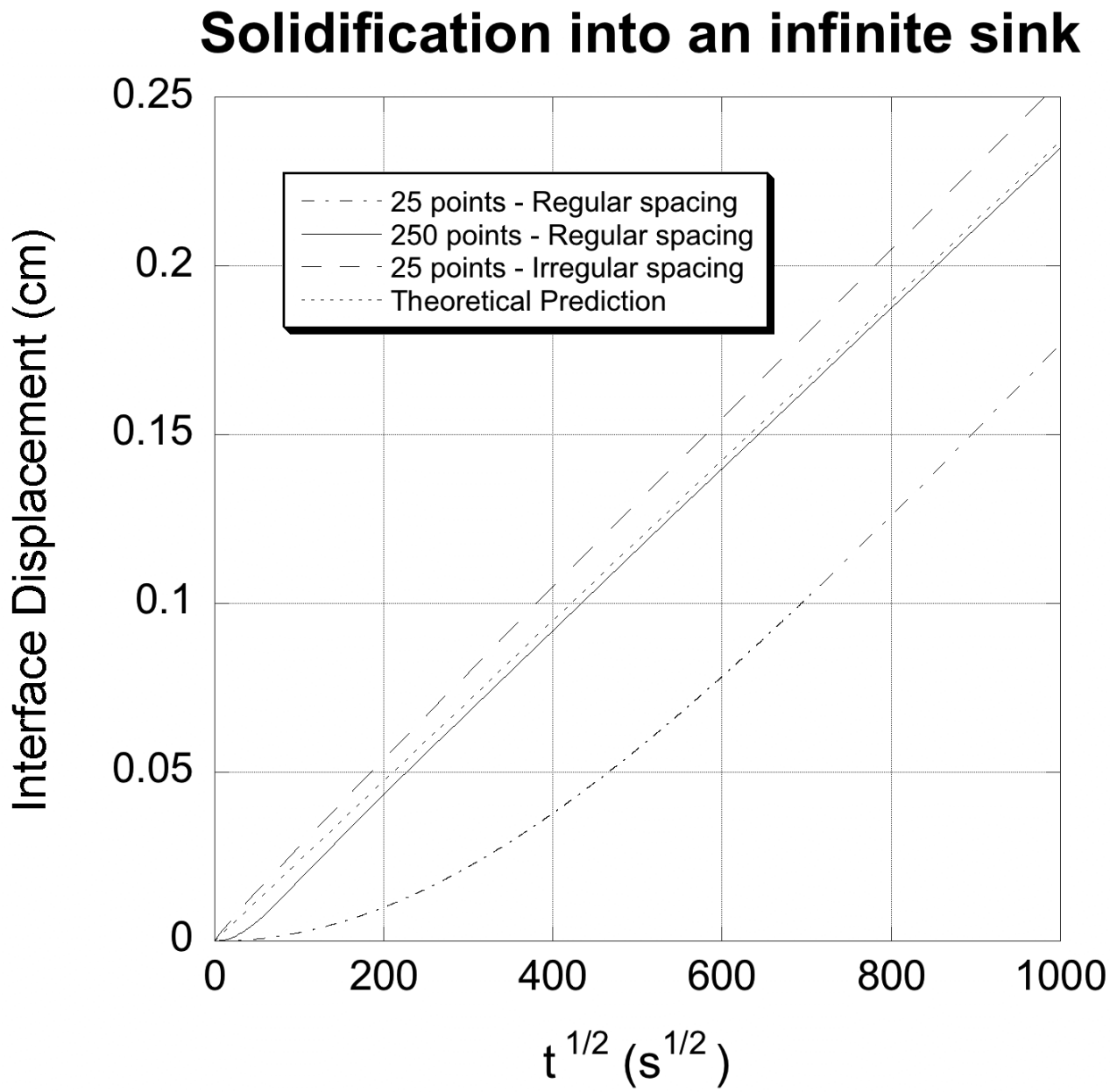

FIGURE 4: Analytical and numerical predictions of interface motion during the diffusion-controlled solidification of a liquid at homogenous composition with an infinitely large sink for the solute. The diffusion coefficient in the solid was taken to be 4.8×10^{-8} $cm^{2}s^{-1}$. *To approximate an infinite sink, numerical results were calculated using* $s(0)=1$ cm *and* $L=10$ cm. *The various results correspond to different spatial discretisations. In each case, a constant timestep (fixed at* $\delta t=1$ sec*) was used. We take* $c_A=0.3$, $c_B=0.2$ *and* $c_\infty=0$. *This corresponds to* $k=-0.54$ *for the analytical solution.*